Published in final edited form as:
Fungal Genet Biol. 2011 February ; 48(2): 154–165. doi:10.1016/j.fgb.2010.10.006.

Ste50 adaptor protein governs sexual differentiation of *Cryptococcus neoformans* via the pheromone response MAPK signaling pathway

Kwang-Woo Jung[a,*], **Seo-Young Kim**[a,*], **Laura H. Okagaki**[b], **Kirsten Nielsen**[b], and **Yong-Sun Bahn**[a,**]

[a] Department of Biotechnology, Center for Fungal Pathogenesis, Yonsei University, Seoul, Korea

[b] Department of Microbiology, Medical School, University of Minnesota, Minneapolis, MN, USA

Abstract

The mitogen-activated protein kinase (MAPK) pathways control diverse cellular functions in pathogenic fungi, including sexual differentiation, stress-response, and maintenance of cell wall integrity. Here we characterized a *C. neoformans* gene, which is homologous to the yeast Ste50 that is known to play an important role in mating pheromone response and stress response as an adaptor protein to the Ste11 MAPK kinase kinase in *Saccharomyces cerevisiae*. The *C. neoformans* Ste50 was not involved in any of the stress responses or virulence factor production (capsule and melanin) that are controlled by the HOG and Ras/cAMP signaling pathways. However, Ste50 was required for mating in both serotype A and serotype D *C. neoformans* strains. The *ste50Δ* mutant was completely defective in cell-cell fusion and mating pheromone production. Double mutation of the *STE50* gene blocked increased production of pheromone and the hyper-filamentation phenotype of cells deleted of the *CRG1* gene, which encodes the RGS protein that negatively regulates pheromone responsive G-protein signaling via the MAPK pathway. Regardless of the presence of the basidiomycota-specific SH3 domains of Ste50 that are known to be required for full virulence of *Ustilago maydis*, Ste50 was dispensable for virulence of *C. neoformans* in a murine model of cryptococcosis. In conclusion, the Ste50 adaptor protein controls sexual differentiation of *C. neoformans* via the pheromone-responsive MAPK pathway but is not required for virulence.

Keywords

Cryptococcus neoformans; MAPK; Ste50; Pheromone; Stress response

1. Introduction

The mitogen-activated protein kinase (MAPK) signaling pathways commonly exist in all eukaryotic organisms and play a wide variety of cellular roles in growth, differentiation, and stress response. All MAPK modules are comprised of three protein kinases: MAPK kinase

**Correspondence to Dr. Yong-Sun Bahn: Department of Biotechnology, Center for Fungal Pathogenesis, Yonsei University, 134 Shinchon-dong, Seodaemun-gu, 120-749, Seoul, Korea, ysbahn@yonsei.ac.kr, Tel: +82-2-2123-5558, Fax: +82-2-362-7265.
*KW Jung and SY Kim equally contributed to this work

kinase (MAPKKK), MAPK kinase (MAPKK), and MAPK. Humans contain three major MAPKs, ERK, JNK, and p38 MAPKs, which are involved in growth, differentiation, immunomodulation, stress response, and apoptosis (Johnson and Lapadat, 2002; Waskiewicz and Cooper, 1995). In fungi, several MAPK signaling pathways have been extensively characterized, including the pheromone response Kss1/Fus3-like MAPK pathway, the stress-activated Hog1-like MAPK pathway, and the cell wall integrity Mpk1-like MAPK pathway. Understanding of these MAPK pathways is particularly important for characterizing growth, differentiation, and virulence features of pathogenic fungi.

Three MAPK signaling pathways have been discovered in *Cryptococcus neoformans*, which causes pulmonary cryptococcosis and meningoencephalitis that is a life-threatening disease if not treated (Idnurm et al., 2005; Lin and Heitman, 2006). One MAPK pathway is mediated by the Cpk1 protein kinase. Disruption of *CPK1* results in defective pheromone production, mating, and monokaryotic fruiting, which are essential for production of infectious spores (Davidson et al., 2000; Davidson et al., 2003; Wang et al., 2004). The Cpk1 MAPK is highly homologous to the Kss1 and Fus3 dual MAPK system that modulates mating and filamentous growth of *S. cerevisiae*. Similar to *S. cerevisiae* and other fungi, Ste11 MAPKKK and Ste7 MAPKK work upstream of the Cpk1 MAPK (Davidson et al., 2003). Upstream of the Cpk1 MAPK module are a pheromone-sensing G-protein coupled receptor Cpr1 (also known as Ste3) and its associated α-subunits (Gpa2 and Gpa3). These two α subunits (Gpa2 and Gpa3) and the β subunit Gpb1 of heterotrimeric GTP-binding protein (G protein) complex are known to be involved in the mating process (Hsueh et al., 2007). Unlike *S. cerevisiae*, however, Ste12 is not a major transcription factor for Cpk1 in *C. neoformans* since it plays only a minor role in mating (Alspaugh et al., 1998; Wickes et al., 1997; Yue et al., 1999).

The second MAPK in *C. neoformans* is an Mpk1 protein kinase, which is required for maintenance of cell wall integrity and growth at high temperature that is critical for *C. neoformans* to survive in the host (Kraus et al., 2003). Mkk1 (also known as Mkk2) MAPKKK and Bck1 MAPKK are two upstream protein kinases for the Mpk1 MAPK (Gerik et al., 2005; Kojima et al., 2006). The Mkk1-Bck1-Mpk1 pathway is activated by protein kinase C (PKC) that responds to cell wall perturbing agents and high temperature (Gerik et al., 2008; Gerik et al., 2005; Kraus et al., 2003). PKC plays an additional role in controlling melanin biosynthesis (Heung et al., 2004).

The third MAPK in *C. neoformans* is the Hog1 stress-activated protein kinase that responds to a variety of environmental stresses, including osmotic changes, oxidative and genotoxic damages, UV irradiation, high temperature, antifungal drugs, toxic metabolites, and heavy metal exposure (Bahn, 2008; Bahn et al., 2007a; Bahn et al., 2005b; Bahn et al., 2006). Hog1 is activated by Pbs2 MAPKK and Ssk2 MAPKKK (Bahn et al., 2007a; Bahn et al., 2005b). Upstream of the Hog1 MAPK module, the two-component-like phosphorelay system, composed of two hybrid sensor kinases (Tco1 and Tco2), a histidine-containing phosphotransfer protein (Ypd1), and two response regulators (Ssk1 and Skn7), relays its signal to Ssk2 (Bahn et al., 2006; Ko et al., 2009). Interestingly, the HOG (High Osmolarity Glycerol response) pathway, consisting of the Hog1 MAPK module and the phosphorelay system, also controls production of two virulence factors, capsule and melanin as well as sexual differentiation, indicating that the Hog1 MAPK pathway cross-talks with other signaling pathways (Bahn, 2008; Bahn et al., 2007a; Bahn et al., 2005b; Bahn et al., 2006). In addition, recent transcriptome analysis revealed that the HOG pathway negatively controls ergosterol biosynthesis, which affects susceptibility to the polyene and azole drugs (Ko et al., 2009).

Although the basic signaling components and regulatory mechanism of each MAPK pathway have been characterized in *C. neoformans*, the potential cross-talk between the MAPK pathways has not been well characterized. Therefore, we aimed to investigate a signaling component that has been reported to link multiple MAPK pathways to other signaling pathways in fungi. The Ste50 adaptor protein is a protein kinase regulator that contains two evolutionarily conserved domains, SAM (Sterile Alpha Motif) and RA (Ras Association), at the amino and carboxy terminals, respectively (O'Rourke and Herskowitz, 1998; Posas et al., 1998). The SAM domain is a protein-binding domain playing a role in signal transduction and transcriptional regulation in eukaryotes (Bhunia et al., 2009; Slaughter et al., 2008). The RA domain is required for proper localization of the cargo proteins that Ste50 delivers (Truckses et al., 2006; Wu et al., 2006). The RA domain of Ste50 in *S. cerevisiae* controls HOG pathway activation for osmoregulation through interaction with the cytoplasmic single-transmembrane protein Opy2 (Ekiel et al., 2009). In *S. cerevisiae*, Ste50 is involved in multiple MAPK signaling pathways, governing mating, filamentous growth, and stress response (Posas et al., 1998; Rad et al., 1992; Ramezani Rad et al., 1998). It acts as an adaptor protein between the G-protein associated Cdc42-Ste20 protein complex and its effector protein Ste11 MAPKKK (O'Rourke and Herskowitz, 1998; Posas et al., 1998). Ste50-binding inhibits the interaction between the regulatory N-terminus and catalytic C-terminus of Ste11, which allows Ste11 to autophosphorylate (Wu et al., 1999). In *S. cerevisiae*, Ste11 MAPKKK regulates multiple MAPK pathways, including the Fus3 MAPK for the mating process, the Kss1 MAPK for filamentous growth, and the Hog1 MAPK for stress response (Lee and Elion, 1999; O'Rourke and Herskowitz, 1998; Posas and Saito, 1997). In addition to its role as an adaptor for Ste11, Ste50 has also been implicated in the Ras-cAMP signaling pathway, possibly due to the presence of the RA domain at the C-terminus (Poplinski et al., 2007; Ramezani-Rad, 2003). Indeed, Ste50 also interacts with Ras1 and Ras2 via the RA domain (Ramezani-Rad, 2003). In contrast to the Ste50 in ascomycota, the Ste50 in basidiomycota contains two additional SH3 domains at the C-terminus (Klosterman et al., 2008). Expectedly, the N-terminal SAM and RA domains are required for filamentous growth of *U. maydis* (Klosterman et al., 2008). Interestingly, the SH3 domains are dispensable for filamentation in *U. maydis* but are required for virulence (Klosterman et al., 2008), indicating that the SH3 domains of Ste50 may play an essential role in pathogenicity of basidiomycete fungal pathogens.

To investigate the role of Ste50 in the *C. neoformans* Cpk1-, Hog1-, and Ras-signaling pathways, we deleted the *STE50* gene and analyzed the mutant for changes in signaling through the MAPK and Ras pathways. Ste50 is dispensable for stress response and production of two major virulence factors, capsule and melanin, indicating that Ste50 is not involved in regulation of the Hog1 and Ras-signaling pathways. However, Ste50 was required for sexual reproduction via the Cpk1 MAPK pathway. In contrast to other ascomycetes and basidiomycetes where Ste50 is involved in multiple signaling pathways, our study demonstrates that the Ste50 in *C. neoformans* is dedicated to control of the pheromone-responsive MAPK pathway.

2. Materials and Methods

2.1. Strains, plasmid, and media

The *C. neoformans* strains used in this study are listed in Table 1 and were cultured in YPD (yeast extract-peptone-dextrose) medium. V8 medium (pH 5.0) (Cambell, Camden, NJ) for mating, agar-based DME (Dulbecco's modified Eagle's) medium (Invitrogen, Carlsbad, CA) for capsule production, and Niger seed or L-DOPA medium for melanin production were prepared as previously described (Bahn et al., 2004).

2.2. cDNA analysis and two-hybrid assay

To perform two-hybrid assay between *C. neoformans* Ste11 and Ste50, first we cloned cDNAs for *STE11* and *STE50* genes. Each cDNA was amplified by RT-PCR using total RNA prepared from matings between JEC21 and JEC20 strains (serotype D *C. neoformans* *MAT*α and *MAT***a** strains, respectively) as a template and primers JOHE11932/JOHE11933 for *STE50* and B2093/B2094 for *STE11* (Table S1). The RT-PCR products were cloned into a pCR2.1-TOPO vector, generating pCR-STE50c and pCR-STE11c, respectively. The cloned cDNA of *STE50* and *STE11* were sequenced and deposited to GenBank (accession number HQ113107 and HQ113108, respectively).

The cDNA fragment of the *STE50* gene was subcloned into plasmid pGBT9 with in-frame fusion to the Gal4 binding domain, generating pGBT-STE50c. The cDNA insert of the *STE11* gene was subcloned into pGAD424 with in-frame fusion to the Gal4 activation domain, generating pGAD-STE11c. The two plasmids, pGBT-STE50c and pGAD-STE11c, were cotransformed into the reporter yeast strain PJ69-4A and at least three independent Leu^+ Trp^+ transformants were selected on SD medium lacking leucine and tryptophan (SD-Leu-Trp). To qualitatively examine protein- interaction, we monitored the growth ability of the transformants on SD-Leu-Trp-His and SD-Leu-Trp-His-Ade media. For quantitative examination, β-galactosidase activity was measured as previously described (Rose and Botstein, 1983). As control plasmids, pGAD-ACA1 and pGBT-$CAC1_{(2126–2260)}$ were used for transformation and yeast two-hybrid assays (data not shown).

2.3. Construction of the ste50Δ mutants

The *STE50* gene (CNAG_07507) were disrupted in the serotype A *MAT*α strain H99, the congenic *MAT***a** strain KN99**a,** and the serotype D *MAT*α strain JEC21 genetic backgrounds with a disruption cassette generated by overlap PCR followed by biolistic transformation, as previously described (Bahn et al., 2005a; Davidson et al., 2002). Primers for amplification of the 5′ and 3′ flanking regions of the serotype A and D *STE50* genes are listed in Supplementary Table S1. M13Re and M13Fe primers were used to amplify the Nat^r or Neo^r dominant selectable marker. Each gel-extracted gene disruption cassette was biolistically transformed into the serotype A strains H99 or KN99**a**, or the serotype D strain JEC21 (Davidson et al., 2000). NAT^r or NEO^r positive stable transformants were selected on YPD medium containing nourseothricin or G418, respectively. To confirm genotype of the *ste50Δ* mutants, both diagnostic PCR and Southern blot analysis were performed (Supplementary Fig. S1 and S2). All PCR amplifications were performed using the ExTaq polymerase (Takara, Shiga, Japan).

To construct the *ste50Δ crg1Δ* double mutant, the *ste50* disruption allele constructed by double joint PCR (DJ-PCR) was biolistically transformed in the *MAT*α *crg1Δ* mutant (H99 crg1) and *MAT***a** *crg1Δ* mutant (PPW 196) strains (Kim et al., 2009). The correct genotype of the *ste50Δ crg1Δ* double mutants was confirmed by diagnostic PCR and Southern blot analysis (Supplementary Fig. S3).

2.4. Construction of the ste50Δ+STE50 complemented strain

To verify the phenotypes of the *ste50*Δ mutants we constructed, the *ste50*Δ*+STE50* complemented strains were generated as follows. First, the full-length *STE50* gene, which contains 895 bp of the 5′-untranslated region (UTR), 2699 bp of the *STE50* open reading frame (ORF), and 168 bp of the 3′-UTR, was amplified by PCR with H99 genomic DNAs as templates and primers B1360 and B1361 containing a NotI recognition site and directly cloned into the TOPO vector (Invitrogen) to generate plasmid pCR-STE50. After confirming the DNA sequence, the *STE50* insert was subcloned into the plasmid pJAF12 (NEO^r) to produce the plasmid pJAF12-STE50. For the targeted re-integration of the wild-

type *STE50* allele into its native locus, pJAF12-STE50 was linearized by NsiI (New England Biolabs) digestion and biolistically transformed into the *ste50*Δ mutant (YSB317).

2.5. Southern blot analysis

Genomic DNAs were isolated from each strain as follows. Cells were grown in YPD medium overnight (50 ml culture), spun-down, and lyophilized. The lyophilized cell pellet was vigorously vortexed with 3 mm glassbeads (Sigmund Lindner) in 10 ml of CTAB (Cetyl trimethylammonium bromide, Sigma) extraction buffer (100 mM Tris-HCl pH7.5, 0.7 M NaCl, 10 mM EDTA, 1% CTAB, 1% β-mercaptoethanol), incubated at 65°C for 30 min, and cooled to room temperature. Then the cell extracts were mixed with 10 ml chloroform and spun down for phase separation. Genomic DNA was precipitated from the aqueous phase with an equal volume of isopropanol, washed with 70% ethanol, and resuspended in TE buffer (10mM Tris and 1mM EDTA) containing RNase H. Isolated genomic DNA was digested with the indicated restriction enzymes (i.e. HindIII for checking deletion of the *STE50* gene in both serotype A and D). The digested genomic DNAs were separated by 1% agarose gel-electrophoresis, denatured in 0.4 N NaOH, transferred to the nylon membrane (GE) in 0.4 N NaOH and 1 M NaCl, and fixed by 1200 J/m^2 UV exposure. The membrane was hybridized with modified church hybridization solution (1mM EDTA, 0.25M Na_2HPO_4, 1% hydrolysated casein, 7% SDS, 6% H3PO4) containing *STE50*-specific probes that were PCR-amplified with primers listed in Supplementary Table 1 and radiolabelled by Amersham Rediprime II Random Prime Labelling System (GE), washed for 10 min with each washing solution I (2×SSC buffer and 0.1% SDS), solution II (2×SSC buffer and 0.1% SDS), and solution III (0.5× SSC buffer and 0.1% SDS), then the membrane was exposed to autoradiography film, overnight.

2.6. Northern blot analysis for monitoring pheromone gene expression during mating

The *MAT*α and *MAT***a** *C. neoformans* strains were grown in YPD medium for 16 hrs at 30°C and equal concentration of cells (10^7 cells/ml) were resuspended in water. The α and **a** mixtures were spread onto V8 medium and incubated in the dark at room temperature for 1 days. Cells were pelleted at 4°C, frozen at −80°C, and lyophilized. Total RNA was isolated using Trizol (Invitrogen). Ten μg of RNA was separated in a 1% agarose gel made with DEPC (diethyl pyrocarbonate)-treated water and 1× MOPS running buffer. The gel was washed three times with distilled water, transferred to a nylon membrane using 20x SSC transfer buffer. The membrane were hybridized with pheromone gene-specific probes that were PCR-amplified with the primers listed in Supplementary Table 1 and radioactively labeled with Rediprime kit (GE), washed and developed as described in for the Southern blot analysis.

2.7. Assays for capsule and melanin production

For capsule induction, each *C. neoformans* strain was incubated for 16 hrs at 30°C in YPD medium, spotted onto agar-based DME medium, and further incubated for 2 days at 37°C. After incubation, capsule production levels were measured qualitatively using India ink staining and quantitatively by comparing the size of capsule for each mutant by microscopically measuring diameters of the capsule and the cell using an Olympus BX51 microscope equipped with a SPOT Insight digital camera (Diagnostic Instrument Inc.) as described previously (Bahn et al., 2004). For additional quantitative measurement of capsule size, packed cell volume was also measured by using hematocrit capillary tubes as described previously (Alspaugh et al., 2002). Briefly, cells grown on DME medium for 2 days were scraped from the medium, washed with PBS (Phosphate buffer saline) to remove released polysaccharide, and fixed with 10% formalin. Cell concentration was determined by using hemocytometer and adjusted to 1×10^9 cells/ml with PBS buffer. Forty microliters of the cell suspension was loaded into Microhematocrit capillary tubes (HIRSCHMANN

LABOGERÄTE No. 9100275 Germany) with clay and parafilm sealed tips to prevent evaporation of the medium during incubation. The capillary tubes were placed vertically overnight at room temperature to allow cell packing by gravity. The packed volume of cells was measured by calculating the ratio of the length of packed cell volume phase/length of total volume phase. Two or three independent triplicate experiments were performed. Statistical difference in relative capsule size between strains was determined by Bonferroni's multiple comparison test by using Prism 4 software (GraphPad Software). For melanin production, cells were spotted onto Niger seed medium or L-DOPA medium containing 0.1% glucose and incubated for up to 7 days at 30°C or 37°C. Melanin production was monitored and photographed daily.

2.8. Mating, cell fusion, and confrontation assays

All *C. neoformans* strains tested for mating, cell fusion, and confrontation assays were initially grown in YPD medium for 16 hrs at 30°C and resuspended in water. For mating, equal concentrations of *MAT*α and *MAT***a** cells (10^7 cells/ml) were mixed, spotted (5 μl) onto V8 mating medium, and incubated in the dark at room temperature for 1 to 2 weeks. The spotted mating mixtures were monitored weekly for filamentation and photographed using an Olympus BX51 microscope equipped with a SPOT Insight digital camera (Diagnostic Instrument Inc.). Cell fusion efficiency was measured as previously described with minor modifications (Bahn et al., 2004). Briefly, 10^7 cells/ml of each *MAT*α and *MAT***a** strain containing Nat^r or Neo^r markers, respectively, were mixed in an equal volume and 5 μl of this cell mixture was spotted onto V8 medium and incubated for 24 hrs at room temperature in the dark. The cells were scraped from the medium, resuspended in 1 ml dH_2O, and 200 μl of cell suspension was plated onto YPD medium containing nourseothricin and G418. The number of colonies on each plate was determined after 4 days of incubation at room temperature. As control strains, YSB119 (Nat^r wild-type strain) and YSB121 (Neo^r wild-type strain) were used. For the confrontation assay to monitor pheromone production and response of cells, α cells were streaked in confrontation with **a** cells on V8 medium and incubated for 10 days at room temperature in the dark. Images of mating and confrontation assays were captured with an Olympus BX51 microscope equipped with a SPOT Insight digital camera (Diagnostic Instrument Inc.).

2.9. Sensitivity test for stress responses

Each strain was incubated overnight (about 16 hrs) at 30°C in YPD medium, serially diluted (1 to 10^4 dilutions) in dH_2O, and spotted (4 μl) onto solid YP or YPD medium. To test osmosensitivity, cells were spotted on YP containing 0.5 M, 1 M, and 1.5 M of NaCl or KCl, or 1.5–2 M sorbitol. To test genotoxic DNA damaging stress, cells were spotted on solid YPD medium and exposed to 200, 300, or 400 J/m^2 of UV by using a UV crosslinker (UVP), or spotted on YPD medium containing 10, 30, 50 mM hydroxyurea (HU) and 0.01, 0.02, 0.03% methylmethane sulfonate (MMS). To test temperature sensitivity, plates were incubated at 25, 30, 37, and 40°C. To examine oxidative stress, cells were spotted on YPD medium containing 2, 3, and 4 mM diamide and 2.5, 3, 3.5 mM hydrogen peroxide (H_2O_2) (Junsei, Tokyo, Japan). To test heavy metal stress and toxic metabolite sensitivity, cells were spotted on YPD medium containing 15, 22.5, and 30 μM cadmium sulfate ($CdSO_4$) (Sigma, Saint Louis, MO) or methylglyoxal (MG). To test cell wall and membrane integrity, cells were spotted on YPD medium containing 0.01, 0.02, and 0.03% sodium dodecyl sulfate (SDS), dithiothreitol (DTT), and 0.2, 0.5, and 0.7% Congo red. To test antifungal drug susceptibility, the cells were spotted on YPD medium containing the indicated concentration of polyene (amphotericin B), azole (fluconazole, ketoconazole, Itraconazole), flucytosine, and phenylpyrrole (fludioxonil) drugs (Sigma). Each plate was incubated for 2–5 days, and photographed during the incubation period.

2.10. Virulence assays

All animal experiments were done at the University of Minnesota in strict accordance with good animal practice as defined by the National Institutes of Health Office of Animal Welfare (OLAW), and the Association for the Assessment and Accreditation of Laboratory Animal Care (AAALAC). All experiments were reviewed and approved by the University of Minnesota Institutional Animal Care and Use Committee (IACUC) under protocol number 0712A22250.

The wild-type strain (H99), *ste50Δ* mutant (YSB317), and its complemented strain (YSB564) were cultured overnight in YPD broth. The resulting yeast cells were pelleted and resuspended in sterile PBS at a concentration of $1x10^6$ cells/ml based on hemocytometer count. Mice were anesthetized by intraperitoneal injection. Animals were infected intranasally with 5×10^4 cells in 50 μl PBS. The concentration of cells in the inoculum was confirmed by plating serial dilutions and enumerating colony forming units (CFUs). Mice were monitored daily and those that showed signs of severe morbidity (weight loss, extension of the cerebral portion of the cranium, abnormal gait, paralysis, seizures, convulsion, or coma) were sacrificed by CO_2 inhalation. Two independent experiments were preformed. In one experiment, groups of ten 6-week-old female C57/BL6 mice (Jackson Laboratories, Bar Harbor, ME) were infected as described above and monitored for time until morbidity. In a second experiment, groups of 7-week-old female A/J mice (Jackson Laboratories, Bar Harbor, ME) (8 mice for the wild-type strain, ten mice for the *ste50Δ* mutant, and six mice for the *ste50Δ+STE50* strain) were infected as described above and monitored for time until morbidity. In this second experiment all mice were included in the survival data presented in Figure 7 as well as for statistical analysis. For statistical test, we used the Mann-Whitney U test (also called the Mann-Whitney-Wilcoxon, the Wilcoxon rank-sum, or the Wilcoxon-Mann-Whitney test), which is a non-parametric significance test. *P*-values <0.05 were considered significant.

To monitor titan cell formation in the wild-type (H99), *ste50Δ* mutant (YSB317), and complemented (YSB564) strains, the yeast cells were resuspended in sterile PBS at a concentration of 2×10^7 cells/ml based on hemocytometer count. Groups of two 7-week-old female A/J mice were anesthetized by intraperitoneal pentobarbital injection. Animals were infected intranasally with 1×10^6 cells in 50 μl PBS. Infected mice were sacrificed at 3 days post-infection by CO_2 inhalation. Lungs were lavaged with 1.5 ml sterile PBS three times using a 20 gauge needle placed in the trachea. Cells in the lavage fluid were pelleted at 16,000g, resuspended in 3.7% formaldehyde, and washed with PBS. >500 cells per animal were analyzed for size by microscopy using an AxioImager microscope (Zeiss, Inc).

3. Results

3.1. Identification of the Ste50 homologue in C. neoformans

To identify the Ste50 ortholog in *C. neoformans*, we performed BLAST searches (tblastn) with the *S. cerevisiae* Ste50 protein sequence. In both serotype A (H99 strain) and D (JEC21 strain), a single Ste50 ortholog was discovered with a relatively low identity (score [Bits] 69.32; E-value, $1.12344e^{-12}$; identity 6.8%). The H99 (CNAG_07507.2) and JEC21 (CNC05800, 179.m00725) *STE50* orthologous genes were predicted to encode proteins of 706 and 700 amino acids (aa), respectively. In order to investigate the detailed genomic structure of the *STE50* gene, we performed cDNA analysis of the *STE50* gene in the JEC21 strain. The cDNA analysis revealed that the open reading frame (ORF) of the *STE50* gene consists of 12 exons and 11 introns and encodes a protein with 700 amino acids, corroborating the prediction from the JEC21 genome database. The predicted genomic structure of the *STE50* gene in the H99 strain also consists of 12 exons and 11 introns

(Broad Institute). Regardless of the low identity and similarity compared with Ste50 orthologs in other fungi, protein domain analysis by Pfam (Wellcome trust Sanger Institute, http://pfam.sanger.ac.uk/) revealed that the predicted *C. neoformans* Ste50 ortholog contains typical Ste50-functional domains, including a SAM (sterile alpha motif) domain at the N-terminal region, a RA (Ras-association) domain in the middle region, and two SH3 domains at the C-terminus (Fig. 1A and 1B). The C-terminal SH3 domains are thought to be basidiomycota-specific, has they have only been identified in Ste50 orthologs of basidiomycetous fungi (Klosterman et al., 2008).

In *S. cerevisiae*, Ste50 regulates a diversity of responses including pheromone response, osmotolerance, and filamentous/invasive growth by interacting with components of the MAPK pathway, including the Ste11 MAPKKK (Posas et al., 1998; Rad et al., 1992; Ramezani Rad et al., 1998). The interaction of Ste50 with Ste11MAPKKK is also well conserved in filamentous fungi (Barr et al., 1996; Wu et al., 1999). Therefore, we examined the Ste50-Ste11 interaction to further confirm that the *C. neoformans* gene (CNC05800 in JEC21 strain or CNAG_07507.2 in H99 strain) is a Ste50 ortholog. Using the full-length cDNA of the *STE50* and *STE11* genes from serotype D JEC21 and JEC20 strains, we constructed pGBT-STE50 and pGAD-STE11 plasmids and performed a yeast two-hybrid assay as described in Materials and Methods. Quantitative measurement of protein interaction by β-galactosidase assay showed that Ste50 interacts with Ste11 in *C. neoformans* (Fig. 2). However, interaction between Ste50 and Ste11 appeared to be weak in *C. neoformans* since the reporter yeast strain PJ69-4A cotransformed with pGBT-STE50 and pGAD-STE11 grew in SD-Leu-Trp-His medium, but not in SD-Leu-Trp-His-Ade medium (data not shown). Interestingly, Ste50 itself has a weak transcriptional activation activity (Fig. 2). Therefore, based on sequence homology and its interaction with Ste11 MAPKKK, we named the *C. neoformans* gene as *STE50*.

3.2. Ste50 is not involved in stress response in C. neoformans

To characterize the function of Ste50 in *C. neoformans*, we constructed *ste50*Δ mutants in the serotype A H99 (*MAT*α) and KN99**a** (*MAT***a**) strains, and the serotype D JEC21 (*MAT*α) strain. The gene disruption cassette was generated by overlap PCR and introduced into each strain by biolistic transformation as described in Materials and Methods. Targeted, non-ectopic, integration of the *STE50*-disruption allele was confirmed by both diagnostic PCR and Southern hybridization (data not shown). To verify phenotypes observed in the *ste50*Δ mutants, we constructed multiple independent *ste50Δ* mutants in each strain background and also constructed *ste50*Δ*+STE50* complemented strains, in which the wild-type *STE50* gene was re-integrated into the native locus of the *STE50* gene as described in Materials and Methods.

Since Ste50 is involved in stress response via the HOG pathway in *S. cerevisiae*, we monitored the capability of the *ste50*Δ mutant to resist a variety of external stresses that are controlled by the HOG pathway in *C. neoformans* (Bahn et al., 2007a; Bahn et al., 2005b; Bahn et al., 2006). Unlike the control HOG pathway mutants, the *ste50*Δ mutant was as resistant to osmotic stress as the wild-type strain (Fig. 3A). Furthermore, Ste50 appeared not to be involved in maintenance of cell wall and membrane integrity and detoxification of toxic metabolite since the *ste50Δ* mutant did not exhibit increased sensitivity to SDS, Congo red, and methylglyoxal (Fig. 3A). In test to monitor oxidative stress response, the *ste50*Δ mutant exhibited WT-levels of resistance to hydrogen peroxide and diamide (Fig. 3B). In contrast, the control *hog1*Δ mutant showed increased sensitivity and resistance to H_2O_2 and diamide, respectively, as reported previously (Fig. 3B). In addition, the *ste50*Δ mutant showed a wild-type response to heavy metal stress. In response to a variety of antifungal drugs, including polyene (amphotericin B), azoles (fluconazole, ketoconazole), and a phenylpyrrole-class fungicide (fludioxonil), the *ste50*Δ mutant exhibited wild-type levels of

sensitivity, which was clearly distinguished from the control HOG pathway mutants (Ko et al., 2009) (Fig. 3C). Furthermore, the *ste50*Δ mutant was as resistant to hydroxyurea and methylmethane sulfonate as the wild-type strain (Fig. 3C and data not shown). Finally, the *ste50*Δ mutant did not exhibit any increased thermosensitivity, in contrast to the control *hog1*Δ mutant. Taken together, Ste50 is not involved in any of the known stress responses in *C. neoformans*.

3.3. The role of Ste50 in melanin and capsule production in C. neoformans

In *C. neoformans*, the HOG pathway mutants, such as *hog1*Δ, *pbs2*Δ, *ssk2*Δ, and *ssk1*Δ mutants, are enhanced in melanin and capsule production by controlling expression of *LAC1* and *CAP10*, *CAP59*, *CAP60*, and *CAP64* genes, respectively (Bahn et al., 2007a; Bahn et al., 2005b; Bahn et al., 2006; Ko et al., 2009). Therefore, we characterized the role of Ste50 for melanin and capsule production of *C. neoformans*. Unlike the control HOG pathway mutants, the *ste50*Δ mutant did not show any enhanced melanin and capsule production (Fig. 4).

3.4. Ste50 is required for sexual reproduction of C. neoformans

The finding that Ste50 is not involved in stress response, including thermotolerance, and virulence factor production, indicates that Ste50 functions independently from the HOG and Ras/cAMP pathways. We addressed whether Ste50 is involved in sexual differentiation of *C. neoformans* via the pheromone-response MAPK pathway since Ste50 is required for filamentous growth of both ascomycete and basidiomycete fungi as an adaptor protein for Ste11-like MAPKKK (Klosterman et al., 2008; Ramezani Rad et al., 1998). Our results clearly demonstrated that Ste50 was required for sexual differentiation of both serotype A and D *C. neoformans*. Even in unilateral crosses with the serotype A wild-type strains (H99 or KN99**a** strain), *ste50Δ* mutants exhibited severe mating defects on V8 mating medium (Fig. 5A). The *ste50*Δ mutant also exhibited a profound mating defect when it is mixed with the serotype D JEC20 (*MAT***a**) strain (data not shown). The mating defect observed in the *ste50*Δ mutant was restored to wild-type levels by introduction of the wild-type *STE50* gene (Fig. 5A), further verifying the role of Ste50 in sexual differentiation.

We also investigated whether Ste50 is required for mating in the serotype D strain. Similar to the serotype A *ste50*Δ mutant, the serotype D *ste50*Δ mutant (JEC21 strain background) exhibited severe mating defects in unilateral crosses with the *MAT***a** JEC20 strain (Fig. 5B). These results strongly indicated that Ste50 is indispensable for sexual reproduction in *C. neoformans* serotype A and D strains.

Next we investigated which mating step is impaired in the *ste50*Δ mutant. Mating in *C. neoformans* is achieved through the following steps. First, two α and **a** cells undergo cellular fusion in response to pheromone and initiate filamentous growth. The two dikaryotic nuclei (α and **a**) progress along the filamentous structure using clamp connections until a basidium is formed and nuclear fusion (karyogamy) occurs. The diploid in the basidium undergoes meiosis to form four chains of basidiospores. As can be seen in Fig. 5, normal filamentous structures were not observed when the *ste50*Δ mutant is mated with wild-type strains, indicating that the *ste50*Δ mutant is impaired at early stages of mating. Therefore, we monitored the ability of the *ste50*Δ mutant to undergo cell fusion. YSB119 (*MAT*α and Nat^r) and YSB121 (*MAT***a** and Neo^r) were used as control strains (Bahn et al., 2004). Both unilateral and bilateral mating crosses between the *MAT*α and Nat^r and *MAT***a** and Neo^r *ste50*Δ mutants were performed (Table 1). Quantitative measurement of Nat^r Neo^r dikaryonic cell fusion products showed that *ste50*Δ mutants did not generate any cell fusion products, indicating that Ste50 is required for the initial cell-to-cell fusion process during mating (Fig. 6A).

Next we addressed whether the defective cell-to-cell fusion results from abnormal cell fusion *per se* or defective pheromone sensing or production. Here we provide several lines of evidence indicating that the defective mating of the *ste50*Δ mutant results from inactivation of pheromone sensing and production. First, mutation of the *STE50* gene blocked induction of pheromone-mediated conjugation tubes in *crg1*Δ mutants, which lack an RGS protein that plays a role in densensitizing the pheromone-responsive pathway (Fig. 6B). *C. neoformans* strains deleted for the *CRG1* gene are hypersensitive to pheromone and form conjugation tubes when *MAT*α and **a** *crg1*Δ mutants are confronted with each other (Nielsen et al., 2003;Wang et al., 2004). When the *MAT*α *ste50Δ crg1Δ* double mutant was confronted by the *MAT***a** *crg1Δ* mutant, neither the *ste50Δ crg1Δ* double mutant nor the *crg1Δ* mutant strains formed conjugation tubes (Fig. 6B). Similarly, the *MAT*α *crg1Δ* mutant did not form conjugation tubes when confronted with the *MAT***a** *ste50Δ crg1Δ* double mutant (Fig. 6B). Second, mutation of *STE50* completely blocked sexual differentiation of the *crg1Δ* mutant in both unilateral and bilateral crosses (Fig. 6C). These data indicate that mutation of *STE50* blocked pheromone production and sensing by the *crg1Δ* mutant, which suggests Ste50 acts downstream of Crg1 in the pheromone-responsive MAPK pathway. Third, expression of the mating pheromone gene (*MFα1*) was strongly repressed by mutation of the *STE50* gene. Transcript levels of *MFα1* in unilateral mating crosses with the *ste50Δ* mutant were dramatically decreased compared to wild-type crosses (Fig. 6D).

Crg1 negatively regulates melanin production under high glucose and temperature (37°C) conditions (Wang et al., 2004) in a manner independent of the pheromone-responsive Cpk1 MAPK pathway. In order to address whether Ste50 also works downstream of Crg1 in a Cpk1-independent manner, we tested whether mutation of *STE50* could suppress the increase in melanin production observed in the *crg1Δ* mutant. We found that mutation of the *STE50* gene was unable to suppress the increased melanin production of the *crg1Δ* mutant (data not shown), indicating that Ste50 acts downstream of Crg1 only for the mating process, but not for the melanin production.

3.5. Ste50 is not required for virulence and titan cell formation in C. neoformans

Ubc2, a Ste50 ortholog in *Ustilago maydis*, not only controls filamentous growth and mating, but also governs pathogenicity through the basidiomycete-specific carboxy terminal extension containing SH3 domains (Klosterman et al., 2008). The fact that *C. neoformans* Ste50 also contains the SH3 domains in the carboxy terminus prompted us to test its role in virulence. We used a murine inhalational model of cryptococosis as described in Materials and Methods. Unlike the *U. maydis ubc2Δ* mutant, the *C. neoformans ste50Δ* mutant was not attenuated in virulence compared to the wild type strain in a C57/BL6 mouse model (Fig. 7A, upper panel). When tested in another mouse genetic background (A/J), the *ste50Δ* mutant and *ste50Δ+STE50* exhibited wild-type levels of virulence (Fig. 7A, lower panel). Therefore, we concluded that Ste50 is not required for virulence of *C. neoformans* regardless of the presence of the basidiomycete-specific SH3 domains in the carboxy terminus.

Pheromone sensing has also been implicated in formation of enlarged cells, known as titan cells, during the pulmonary infection (Okagaki et al., 2010; Zaragoza et al., 2010). Because Ste50 is required for mating and morphological differentiation, we tested the *ste50*Δ mutation for its affect on titan cell formation. The wild-type (H99) and *ste50*Δ mutant strains all showed equivalent levels of titan cell formation 3 days post-infection (Fig. 7B), which suggests Ste50 is not involved in titan cell formation and likely acts further downstream in the mating pathway.

4. Discussion

The present study aimed to identify and functionally characterize a key signaling mediator that contributes to cross-talk between signaling pathways in *C. neoformans*. For this purpose, we chose to investigate the role of the Ste50 adaptor protein in *C. neoformans* because Ste50 is known to be involved in multiple signaling pathways in the budding model yeast *S. cerevisiae*. In *S. cerevisiae*, Ste50 is involved in filamentous growth and cell wall integrity signaling via the Ste11-dependent pathway (Lee and Elion, 1999; Ramezani Rad et al., 1998), osmoadaptation signaling via the HOG pathway (O'Rourke and Herskowitz, 1998; Posas et al., 1998), and stress-tolerance signaling by interacting with the Ras-cAMP signaling pathway (Poplinski et al., 2007). These multiple functions of Ste50 are potentially due to the presence of SAM (Sterile-Alpha-Motif) and RA (Ras-Association) domains in the adaptor protein. Recently, Klosterman and co-workers reported that the Ste50 ortholog in basidiomycete fungi is further extended at the C-terminus and contains additional functional domains, such as SH3 domain (Klosterman et al., 2008). Notably, Ubc2, a Ste50 ortholog in *U. maydis*, also controls virulence of the plant fungus through the SH3 domains in the carboxy terminus, but in a manner independent from the SAM or RA domain in the amino terminus (Klosterman et al., 2008). At this point, however, a signaling cascade(s) governed by the SH3 domain of Ubc2 has not been elucidated.

Our study, however, demonstrates that the function of Ste50 in *C. neoformans* is restricted to mating/filamentous growth. In *C. neoformans*, Ste50 does not play a role in stress responses and virulence factor production that are known to be controlled by the HOG and Ras/cAMP signaling pathways (Alspaugh et al., 2000; Bahn, 2008; Bahn et al., 2007b; Ko et al., 2009; Pukkila-Worley and Alspaugh, 2004). The HOG pathway not only controls resistance of *C. neoformans* against diverse stresses, such as osmotic shock, oxidative and heavy metal stress, UV irradiation, DNA damages, and antifungal drug or toxic metabolite treatment, but also regulates sexual reproduction and production of virulence factors such as capsule and melanin (Bahn, 2008; Ko et al., 2009; Maeng et al., 2010). Besides mating and filamentous growth, however, none of phenotypes related to the HOG-signaling pathway were observed in the *ste50Δ* mutant. Supporting these data, our previous study demonstrates that the Ste11 MAPKKK, which is a Ste50-binding protein in *S. cerevisiae*, is not involved in activation of the HOG-signaling pathway in *C. neoformans* (Bahn et al., 2007a). In the model yeast, the Ste11 MAPKKK is activated by the Sho1 transmembrane protein with the help of Ste50 and subsequently activates the Pbs2-Hog1 MAPK pathway to counteract osmotic stress (Posas et al., 1998). However, *C. neoformans* does not have any proteins homologous to Sho1 in its genome. These observations combined with our previous study further indicate that the Ste50-Ste11 signaling pathway does not activate the Pbs2-Hog1 signaling pathway in *C. neoformans*. In *C. neoformans*, the Ras- and cAMP-signaling pathways also control cell survival under a plethora of environmental stresses, mating, and virulence factor production with some connection to the HOG pathway (Bahn, 2008; Maeng et al., 2010). However, none of the Ras- and cAMP-signaling related phenotypes, except mating, were observed in the *ste50*Δ mutant in *C. neoformans*.

The involvement of Ste50 in mating and filamentous growth of *C. neoformans* appears to be mainly mediated by the pheromone-responsive Ste11-Ste7-Cpk1 MAPK signaling pathway based on several findings made by the present study. First, Ste50 weakly interacts with Ste11 based on the results of a yeast two-hybrid assay. Second, similar to the *ste11*Δ mutant, the *ste50Δ* mutant did not exhibit any filamentation, even in a unilateral cross with the wild-type strain. The HOG pathway mutants, such as *hog1*Δ, *pbs2*Δ, *ssk2*Δ, or *ssk1*Δ mutants, show enhanced mating (Bahn et al., 2007a; Bahn et al., 2005b; Bahn et al., 2006). The cAMP mutants, such as *aca1*Δ, *gpa1*Δ, or *cac1*Δ mutants, are only partially impaired in the unilateral mating cross (Bahn et al., 2004). Third, the *ste50*Δ mutant was almost completely

defective in producing mating pheromone and cell fusion in response to a mating partner, indicating that Ste50 is required for pheromone production. Fourth, mutation of *STE50* can suppress phenotypes, such as enhanced pheromone production/sensing and mating, of the *crg1Δ* mutant. Taken together, these data suggest that Ste50 is one of the signaling components in the pheromone-responsive Cpk1 MAPK pathway.

The unique presence of the C-terminal SH3 domains in the Ste50 orthologs of basidiomycete fungi, including *C. neoformans*, suggests that Ste50 may have specialized functions in the basidiomycota, which have not been noticed in other fungi. Besides this study, the only functional study of Ste50 in the basidiomycota is done in *U. maydis* by Klosterman and co-workers (Klosterman et al., 2008). The Ste50 ortholog in *U. maydis*, Ubc2 adaptor protein, interacts with the Ubc4 MAPKKK, a Ste11 ortholog, and is involved in mating and filamentous growth through the SAM and RA domains. Surprisingly, while the two C-terminal SH3 domains are dispensable for mating, they are required for pathogenicity of *U. maydis*, strongly indicating that Ubc2 has a specialized function in virulence of this important fungal pathogen (Klosterman et al., 2008). In contrast, our study demonstrates that the role of the SH3 domains of Ste50 in fungal virulence is not a generalized phenomenon in the basidiomycota. In *C. neoformans*, the *ste50*Δ mutant exhibited wild-type levels of virulence in two independent mouse genetic backgrounds (A/J and C57/BL6 mice). Furthermore, Ste50 was not required for titan cell formation, which has been observed to occur during host infection of *C. neoformans* (Okagaki et al., 2010; Zaragoza et al., 2010). Taken together, these data indicate that Ste50 is not required for full virulence in this pathogen.

To the best of our knowledge, the function of Ste50 has never been reported in human fungal pathogens. For example, *Candida albicans* contains a single Ste50 ortholog (Orf19.1636), whose function is not known. However, the functional Ste50 binding partner, Ste11 MAPKKK, has been reported in *C. albicans* and *C. glabrata. C. albicans* Ste11 is not involved in stress responses but controls the cell wall damage stress response whereas *C. glabrata* Ste11 is required for hypotonic adaptation, mating response and virulence (Calcagno et al., 2005; Cheetham et al., 2007). Furthermore, ,functions of other signaling components, Cek1 (Cpk1 or Kss1/Fus3 MAPK ortholog), Hst7 (Ste7 MAPKK ortholog), and Cst20 (Ste20 ortholog), in the corresponding MAPK pathway have been characterized in *C. albicans*. The Cst20-Hst7-Cek1 MAPK pathway controls morphological transitions of *C. albicans* under certain filamentation inducing conditions via the Cph1 (Ste12 ortholog) transcription factor (Csank et al., 1998; Leberer et al., 1996). Interestingly, the role of each signaling components in pathogenicity of *C. albicans* is rather different. The *hst7*Δ and *cph1*Δ mutants exhibit WT-levels of virulence. In contrast, the *cst20*Δ or *cek1*Δ mutant show attenuated virulence (Csank et al., 1998; Leberer et al., 1996). These data suggest the role of Ste50 in virulence of *C. albicans* may reveal further differences in Ste50 activity in the pathogenic fungus. Similarly, *A. fumigatus* also contains a single Ste50 (Afu2g17130) and yet its role is not known. Therefore, the role of Ste50 in virulence and differentiation of human pathogenic fungi needs to be further studied.

In conclusion, the present study identified and functionally characterized the Ste50 ortholog in *C. neoformans*. Ste50 is involved in pheromone production/sensing and mating processes via the Cpk1 MAPK pathway, but not in diverse stress responses and virulence factor production.

Supplementary Material

Refer to Web version on PubMed Central for supplementary material.

Acknowledgments

This work was supported by Pioneer Research Center Program through the National Research Foundation of Korea funded by Ministry of Education, Science and Technology (No. 2009-0081512), the National Research Foundation of Korea (NRF) grant funded by the Korea government (MEST) (2009-0063344) (to YSB), and the National Institute of Allergy and Infectious Diseases (NIH) K22 grant AI070152 (to KN).

References

Alspaugh JA, et al. *RAS1* regulates filamentation, mating and growth at high temperature of *Cryptococcus neoformans*. Mol Microbiol 2000;36:352–65. [PubMed: 10792722]

Alspaugh JA, et al. Signal transduction pathways regulating differentiation and pathogenicity of *Cryptococcus neoformans*. Fungal Genet Biol 1998;25:1–14. [PubMed: 9806801]

Alspaugh JA, et al. Adenylyl cyclase functions downstream of the Gα protein Gpa1 and controls mating and pathogenicity of *Cryptococcus neoformans*. Eukaryot Cell 2002;1:75–84. [PubMed: 12455973]

Bahn YS. Master and Commander in fungal pathogens: The two-component system and the HOG signaling pathway. Eukaryot Cell 2008;7:2017–2036. [PubMed: 18952900]

Bahn YS, et al. Carbonic anhydrase and CO_2 sensing during *Cryptococcus neoformans* growth, differentiation, and virulence. Curr Biol 2005a;15:2013–20. [PubMed: 16303560]

Bahn YS, et al. Ssk2 mitogen-activated protein kinase kinase kinase governs divergent patterns of the stress-activated Hog1 signaling pathway in *Cryptococcus neoformans*. Eukaryot Cell 2007a; 6:2278–89. [PubMed: 17951522]

Bahn YS, et al. Adenylyl cyclase-associated protein Aca1 regulates virulence and differentiation of *Cryptococcus neoformans* via the cyclic AMP-protein kinase A cascade. Eukaryot Cell 2004;3:1476–91. [PubMed: 15590822]

Bahn YS, et al. Specialization of the HOG pathway and its impact on differentiation and virulence of *Cryptococcus neoformans*. Mol Biol Cell 2005b;16:2285–300. [PubMed: 15728721]

Bahn YS, et al. A unique fungal two-component system regulates stress responses, drug sensitivity, sexual development, and virulence of *Cryptococcus neoformans*. Mol Biol Cell 2006;17:3122–35. [PubMed: 16672377]

Bahn YS, et al. Sensing the environment: lessons from fungi. Nat Rev Microbiol 2007b;5:57–69. [PubMed: 17170747]

Barr MM, et al. Identification of Ste4 as a potential regulator of Byr2 in the sexual response pathway of *Schizosaccharomyces pombe*. Mol Cell Biol 1996;16:5597–603. [PubMed: 8816472]

Bhunia A, et al. NMR structural studies of the Ste11 SAM domain in the dodecyl phosphocholine micelle. Proteins 2009;74:328–43. [PubMed: 18618697]

Calcagno AM, et al. *Candida glabrata* Ste11 is involved in adaptation to hypertonic stress, maintenance of wild-type levels of filamentation and plays a role in virulence. Med Mycol 2005;43:355–64. [PubMed: 16110782]

Cheetham J, et al. A single MAPKKK regulates the Hog1 MAPK pathway in the pathogenic fungus *Candida albicans*. Mol Biol Cell 2007;18:4603–14. [PubMed: 17804815]

Csank C, et al. Roles of the *Candida albicans* mitogen-activated protein kinase homolog, Cek1p, in hyphal development and systemic candidiasis. Infect Immun 1998;66:2713–2721. [PubMed: 9596738]

Davidson RC, et al. A PCR-based strategy to generate integrative targeting alleles with large regions of homology. Microbiology 2002;148:2607–15. [PubMed: 12177355]

Davidson RC, et al. Gene disruption by biolistic transformation in serotype D strains of *Cryptococcus neoformans*. Fungal Genet Biol 2000;29:38–48. [PubMed: 10779398]

Davidson RC, et al. A MAP kinase cascade composed of cell type specific and non-specific elements controls mating and differentiation of the fungal pathogen *Cryptococcus neoformans*. Mol Microbiol 2003;49:469–85. [PubMed: 12828643]

Ekiel I, et al. Binding the atypical RA domain of Ste50p to the unfolded Opy2p cytoplasmic tail is essential for the high-osmolarity glycerol pathway. Mol Biol Cell 2009;20:5117–26. [PubMed: 19846660]

Gerik KJ, et al. *PKC*1 is essential for protection against both oxidative and nitrosative stresses, cell integrity, and normal manifestation of virulence factors in the pathogenic fungus *Cryptococcus neoformans*. Eukaryot Cell 2008;7:1685–98. [PubMed: 18689526]

Gerik KJ, et al. Cell wall integrity is dependent on the *PKC1* signal transduction pathway in *Cryptococcus neoformans*. Mol Microbiol 2005;58:393–408. [PubMed: 16194228]

Heung LJ, et al. The sphingolipid pathway regulates Pkc1 through the formation of diacylglycerol in *Cryptococcus neoformans*. J Biol Chem 2004;279:21144–53. [PubMed: 15014071]

Hsueh YP, et al. G protein signaling governing cell fate decisions involves opposing Galpha subunits in *Cryptococcus neoformans*. Mol Biol Cell 2007;18:3237–49. [PubMed: 17581859]

Idnurm A, et al. Deciphering the model pathogenic fungus *Cryptococcus neoformans*. Nat Rev Microbiol 2005;3:753–64. [PubMed: 16132036]

Johnson GL, Lapadat R. Mitogen-activated protein kinase pathways mediated by ERK, JNK, and p38 protein kinases. Science 2002;298:1911–2. [PubMed: 12471242]

Kim MS, et al. An efficient gene disruption method in *Cryptococcus neoformans* by double-joint PCR with *NAT*-split markers. Biochem Biophys Res Commun 2009;390:983–988. [PubMed: 19852932]

Klosterman SJ, et al. Ubc2, an ortholog of the yeast Ste50p adaptor, possesses a basidiomycete-specific carboxy terminal extension essential for pathogenicity independent of pheromone response. Mol Plant Microbe Interact 2008;21:110–21. [PubMed: 18052888]

Ko YJ, et al. Remodeling of global transcription patterns of *Cryptococcus neoformans* genes mediated by the stress-activated HOG signaling pathways. Eukaryot Cell 2009;8:1197–1217. [PubMed: 19542307]

Kojima K, et al. Calcineurin, Mpk1 and Hog1 MAPK pathways independently control fludioxonil antifungal sensitivity in *Cryptococcus neoformans*. Microbiology 2006;152:591–604. [PubMed: 16514140]

Kraus PR, et al. The *Cryptococcus neoformans* MAP kinase Mpk1 regulates cell integrity in response to antifungal drugs and loss of calcineurin function. Mol Microbiol 2003;48:1377–87. [PubMed: 12787363]

Leberer E, et al. Signal transduction through homologs of the Ste20p and Ste7p protein kinases can trigger hyphal formation in the pathogenic fungus *Candida albicans*. Proc Natl Acad Sci U S A 1996;93:13217–22. [PubMed: 8917571]

Lee BN, Elion EA. The MAPKKK Ste11 regulates vegetative growth through a kinase cascade of shared signaling components. Proc Natl Acad Sci U S A 1999;96:12679–84. [PubMed: 10535982]

Lin X, Heitman J. The biology of the *Cryptococcus neoformans* species complex. Annu Rev Microbiol 2006;60:69–105. [PubMed: 16704346]

Maeng S, et al. Comparative transcriptome analysis reveals novel roles of the Ras and cyclic AMP signaling pathways in environmental stress response and antifungal drug sensitivity in *Cryptococcus neoformans*. Eukaryot Cell 2010;9:360–78. [PubMed: 20097740]

Moore TD, Edman JC. The alpha-mating type locus of *Cryptococcus neoformans* contains a peptide pheromone gene. Mol Cell Biol 1993;13:1962–70. [PubMed: 8441425]

Nielsen K, et al. Sexual cycle of *Cryptococcus neoformans* var. *grubii* and virulence of congenic a and α isolates. Infect Immun 2003;71:4831–41. [PubMed: 12933823]

O'Rourke SM, Herskowitz I. The Hog1 MAPK prevents cross talk between the HOG and pheromone response MAPK pathways in *Saccharomyces cerevisiae*. Genes Dev 1998;12:2874–86. [PubMed: 9744864]

Okagaki LH, et al. Cryptococcal cell morphology affects host cell interactions and pathogenicity. PLoS Pathog 2010;6:e1000953. [PubMed: 20585559]

Perfect JR, et al. Karyotyping of *Cryptococcus neoformans* as an epidemiological tool. J Clin Microbiol 1993;31:3305–9. [PubMed: 8308124]

Poplinski A, et al. Ste50 adaptor protein influences Ras/cAMP-driven stress-response and cell survival in *Saccharomyces cerevisiae*. Curr Genet 2007;51:257–68. [PubMed: 17318632]

Posas F, Saito H. Osmotic activation of the HOG MAPK pathway via Ste11p MAPKKK: scaffold role of Pbs2p MAPKK. Science 1997;276:1702–5. [PubMed: 9180081]

Posas F, et al. Requirement of STE50 for osmostress-induced activation of the STE11 mitogen-activated protein kinase kinase kinase in the high-osmolarity glycerol response pathway. Mol Cell Biol 1998;18:5788–96. [PubMed: 9742096]

Pukkila-Worley R, Alspaugh JA. Cyclic AMP signaling in *Cryptococcus neoformans*. FEMS Yeast Res 2004;4:361–7. [PubMed: 14734016]

Rad MR, et al. *STE50*, a novel gene required for activation of conjugation at an early step in mating in *Saccharomyces cerevisiae*. Mol Gen Genet 1992;236:145–54. [PubMed: 1494345]

Ramezani-Rad M. The role of adaptor protein Ste50-dependent regulation of the MAPKKK Ste11 in multiple signalling pathways of yeast. Curr Genet 2003;43:161–70. [PubMed: 12764668]

Ramezani Rad M, et al. Ste50p is involved in regulating filamentous growth in the yeast *Saccharomyces cerevisiae* and associates with Ste11p. Mol Gen Genet 1998;259:29–38. [PubMed: 9738877]

Rose M, Botstein D. Construction and use of gene fusions to lacZ (beta-galactosidase) that are expressed in yeast. Methods Enzymol 1983;101:167–80. [PubMed: 6310320]

Slaughter BD, et al. SAM domain-based protein oligomerization observed by live-cell fluorescence fluctuation spectroscopy. PLoS One 2008;3:e1931. [PubMed: 18431466]

Truckses DM, et al. The RA domain of Ste50 adaptor protein is required for delivery of Ste11 to the plasma membrane in the filamentous growth signaling pathway of the yeast *Saccharomyces cerevisiae*. Mol Cell Biol 2006;26:912–28. [PubMed: 16428446]

Wang P, et al. Mutation of the regulator of G protein signaling Crg1 increases virulence in *Cryptococcus neoformans*. Eukaryot Cell 2004;3:1028–35. [PubMed: 15302835]

Waskiewicz AJ, Cooper JA. Mitogen and stress response pathways: MAP kinase cascades and phosphatase regulation in mammals and yeast. Curr Opin Cell Biol 1995;7:798–805. [PubMed: 8608010]

Wickes BL, et al. The *Cryptococcus neoformans STE12*α gene: a putative *Saccharomyces cerevisiae STE12* homologue that is mating type specific. Mol Microbiol 1997;26:951–60. [PubMed: 9426132]

Wu C, et al. Adaptor protein Ste50p links the Ste11p MEKK to the HOG pathway through plasma membrane association. Genes Dev 2006;20:734–46. [PubMed: 16543225]

Wu C, et al. Functional characterization of the interaction of Ste50p with Ste11p MAPKKK in *Saccharomyces cerevisiae*. Mol Biol Cell 1999;10:2425–40. [PubMed: 10397774]

Yue C, et al. The STE12α homolog is required for haploid filamentation but largely dispensable for mating and virulence in *Cryptococcus neoformans*. Genetics 1999;153:1601–15. [PubMed: 10581270]

Zaragoza O, et al. Fungal cell gigantism during mammalian infection. PLoS Pathog 2010;6:e1000945. [PubMed: 20585557]

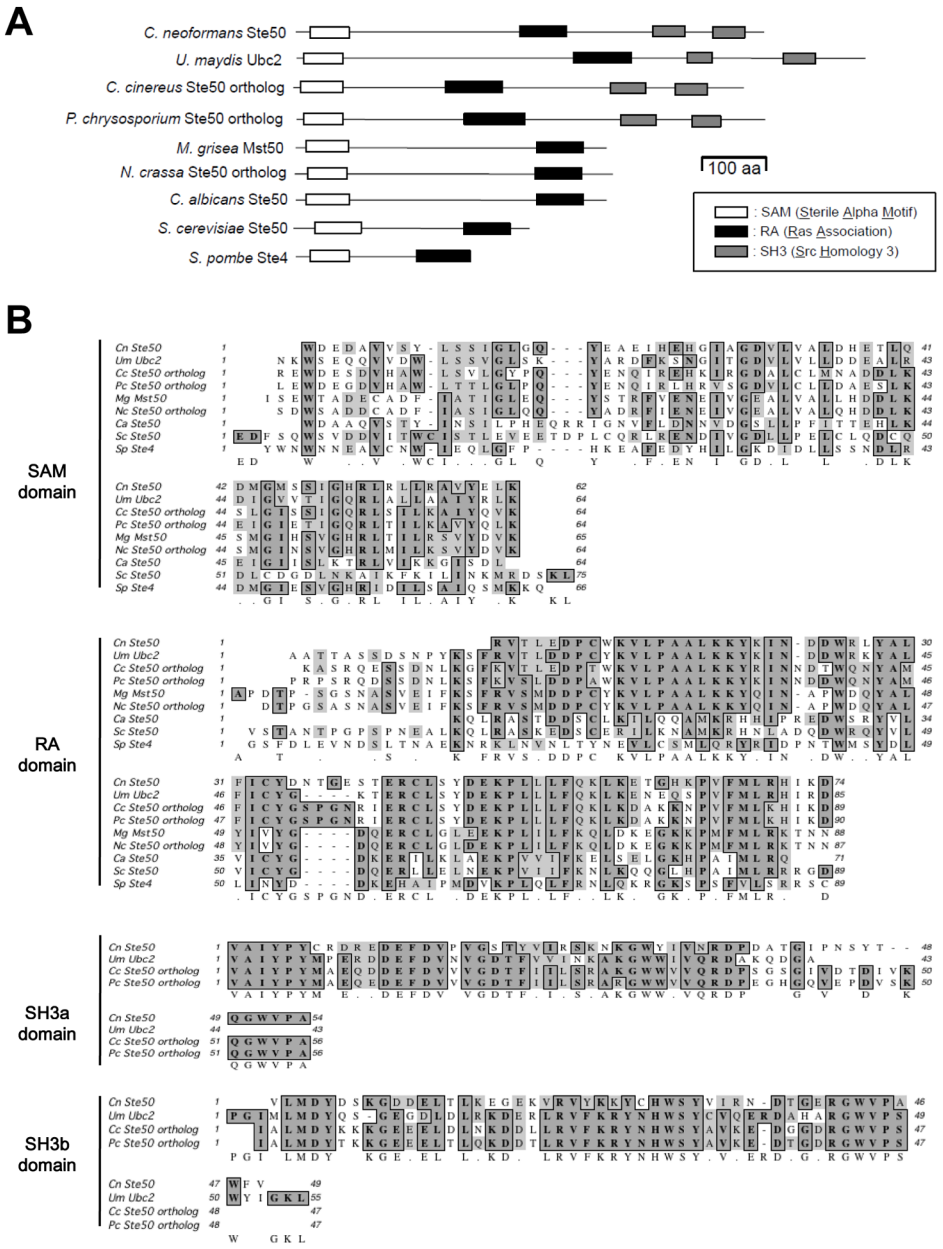

Fig. 1.

Comparison of Ste50 orthologs between *C. neoformans* and other fungi. (A) Each Ste50 ortholog diagram shows functional protein domains, which were identified by the Pfam 24.0 database (http://pfam.sanger.ac.uk/). Each domain indicates the following: SAM, sterile alpha motif; RA, Ras- associated; SH3, Src homology 3. (B) Multiple sequence alignment of Ste50 orthologs is depicted by Clustal W alignment from MacVector software (versions 7.2.3, Accelrys). Protein sequences of Ste50 orthologs were retrieved from the following database: *C. neoformans* Ste50 - CNAG_07507 from the *C. neoformans var. grubii* H99 database of the Broad Institute (http://www.broadinstitute.org/annotation/genome/cryptococcus_neoformans/MultiHome.html); *Ustilago maydis* Ubc2 - GenBank accession number AAK4932; *Coprinus cinereus* - locus CC1G_00975.3 from the *C. cinereus* Sequencing Project

Database of the Broad Institute. (http://www.broadinstitute.org/annotation/genome/coprinus_cinereus/MultiHome.html); *Phanerochaete chrysosporium* Ste50 ortholog - protein ID 2321 at locus Phchr1/scaffold_3:1012644-101605 from the sequencing data produced by the United States Department of Energy, Joint Genome Institute (http://genome.jgi-psf.org/Phchr1/Phchr1.home.html); *Neurospora crassa* Ste50 ortholog - GenBank accession number XP_956774; *Magnaporthe grisae* Mst50 - GenBank accession number XP_359578; *Candida albicans* Ste50 - GenBank accession number XP_721713; *Saccharomyces cerevisiae* Ste50 - GenBank accession number NP_009898; *Schizosaccharomyces pombe* Ste4; GenBank accession number CAB38684.

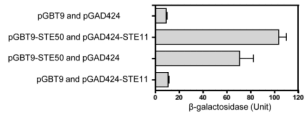

Fig. 2.

Ste50 interacts with Ste11 in *C. neoformans*. Two-hybrid assay was performed with *C. neoformans* Ste50 and Ste11. β-galactosidase activity of a LacZ reporter gene in the PJ69-4A strain co-transformed with indicated vectors were measured with extracts of two independent Leu^+ Trp^+ transformants cultured in SD-Leu-Trp medium. Error bar indicates standard deviation.

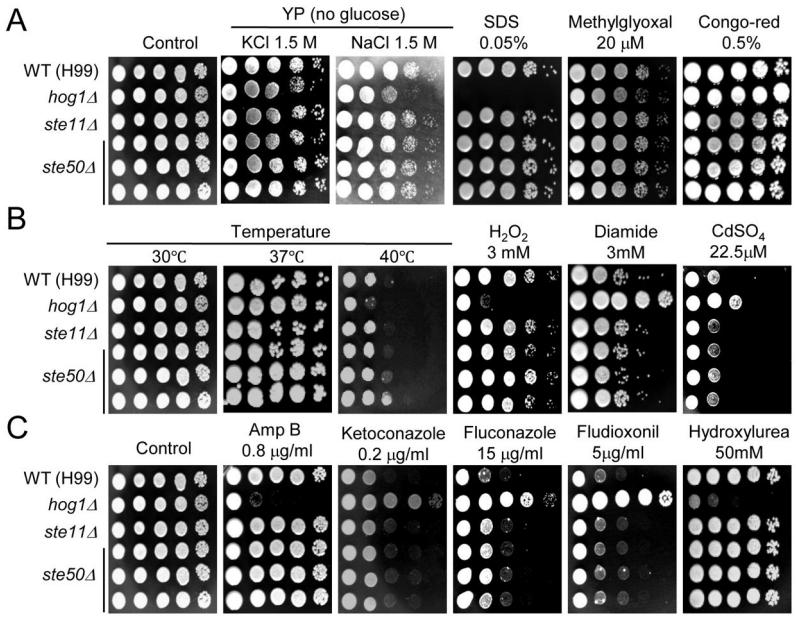

Fig. 3.

Ste50 is not involved in the *C. neoformans* stress response. *C. neoformans* strains (the wild-type strain H99 and *hog1*Δ (YSB64), *ste11*Δ (YSB313), and *ste50*Δ (YSB317, YSB318, and YSB319) mutants) was grown overnight at 30°C in liquid YPD medium, 10-fold serially diluted ($1–10^4$ dilutions), and spotted (3 μl of dilution) on YPD or YP agar containing the indicated concentrations of KCl, NaCl, SDS, Methylglyoxal, Congo red (A), hydrogen peroxide (H_2O_2), diamide, $CdSO_4$ (B), amphotericin B, ketoconazole, fluconazole, fludioxonil, and hydroxyurea (C). Cells were incubated at 30°C for 72 h and photographed. For the thermotolerance test (B), cells were spotted on YPD medium and incubated at 40°C for 4 days.

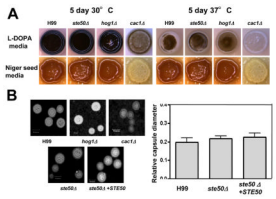

Fig. 4.

Ste50 is not involved in capsule and melanin production of *C. neoformans*. (A) The following strains were spotted and grown on L-DOPA medium (glucose 0.1%) and Niger seed medium (glucose 0.1%) at 30°C or 37°C for 5 days: WT (H99) and *ste50*Δ (YSB317), *hog1*Δ (YSB64) and *cac1*Δ (YSB42) mutant strains. (B) The WT strain H99, *hog1*Δ (YSB64), *cac1*Δ (YSB42), *ste50*Δ (YSB317) and *ste50*Δ + *STE50* (YSB564) strains were spotted and cultured on DME medium for capsule production at 37°C for 2 days. Cells were scraped, resuspended in distilled water, and visualized by India ink staining The packed volume of the cells (the wild-type strain [H99] and *ste50Δ* [YSB317] and *ste50Δ + STE50* [YSB564] strains) was measured by calculating the ratio of the length of packed cell volume phase/length of total volume phase. Statistical differences in relative capsule size between strains was determined by Bonferroni's multiple comparison test.

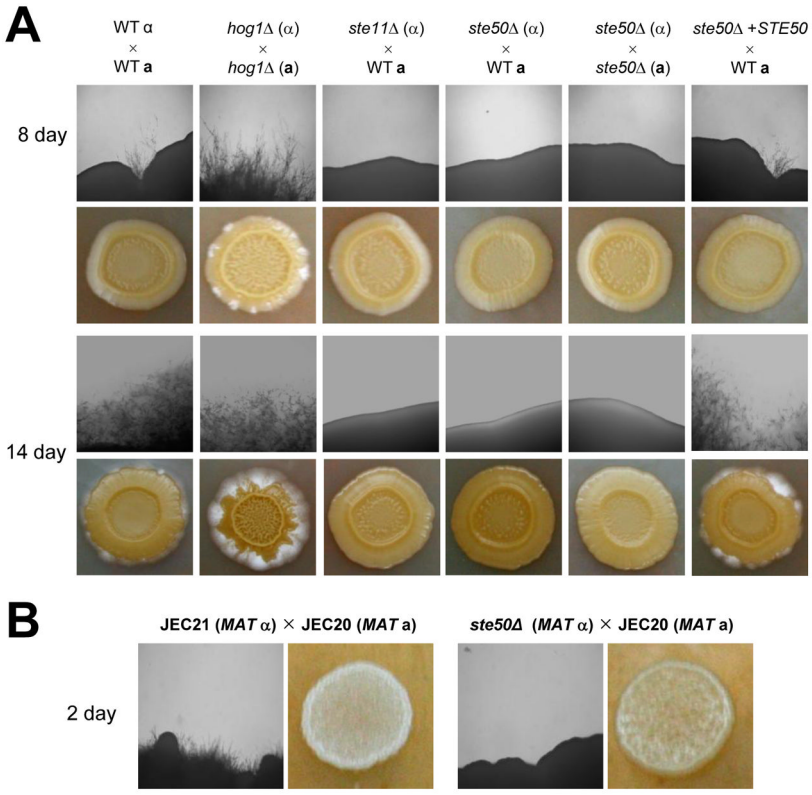

Fig. 5.

Ste50 is required for sexual differentiation in both serotype A and serotype D *C. neoformans* strains. (A) Serotype A *MAT*α and *MAT***a** strains were co-cultured on V8 medium (pH 5.0) for 2 weeks at room temperature in the dark: WT α × WT **a (**H99 and KN99), *hog1Δ* (α) × *hog1Δ* (**a)** (YSB64 and YSB81), *ste11Δ* (α)× WT (**a**) (YSB313 and KN99), *ste50Δ* (α) × WT (**a**) (YSB317 and KN99), *ste50Δ* (α) × *ste50Δ* (**a**) (YSB317 and YSB523), and *ste50Δ* + *STE50* (α) × WT (**a**) (YSB564 and KN99). The images were photographed after 8 days and 14 days. (B) The following serotype D strains were co-cultured on V8 medium in the dark at room temperature up to 5 days and photographed after 2 days: JEC21 and JEC20 (α × **a**), YSB593 and JEC20 (*ste50Δ* × **a**)

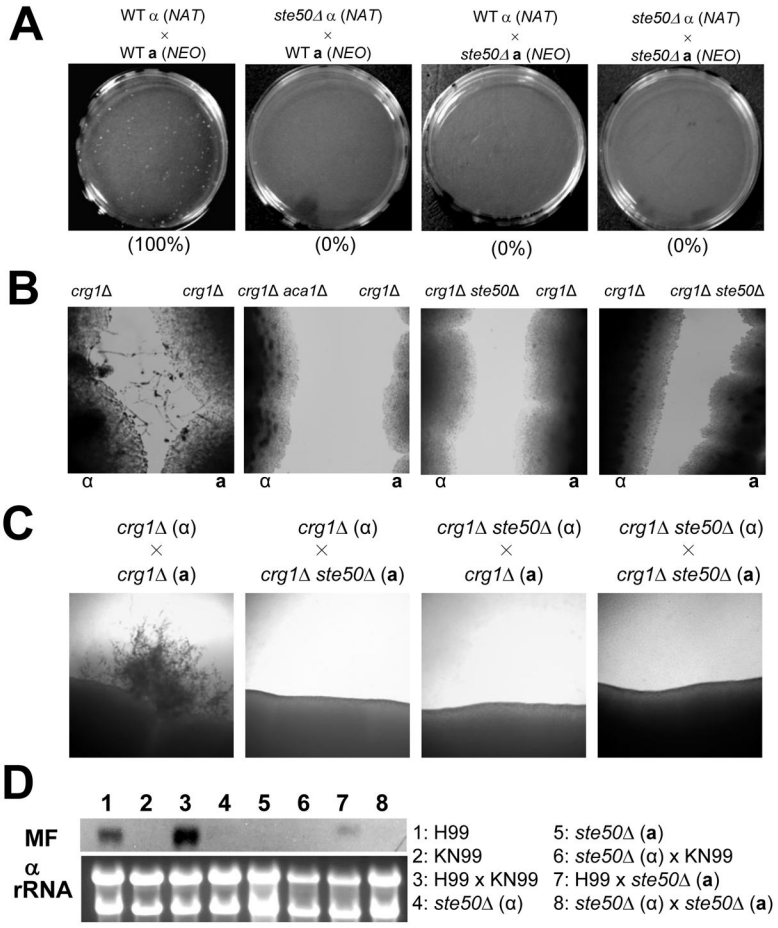

Fig. 6.

Ste50 governs sexual differentiation via the pheromone-responsive Cpk1 MAPK pathway. (A) Cell-cell fusion assays were performed with the following strains: WT α (*NAT*) × WT **a** (*NEO*) (YSB119 and YSB121), *ste50Δ* α (*NAT*) × WT **a** (*NEO*) (YSB317 and YSB121), WT α (*NAT*) × *ste50Δ* **a** (*NEO*) (YSB119 and YSB522), *ste50Δ* α (*NAT*) × *ste50Δ* **a** (*NEO*) (YSB317 and YSB522). Cell fusion efficiency for each experimental set was calculated relative to the control strains (WT α (*NAT*) × WT **a** (*NEO*)). (B) Confrontation assays were performed with the following strains: *MAT*α *crg1Δ* (H99 crg1), *MAT***a** *crg1Δ* (PPW 196), *MAT*α *crg1Δ aca1Δ* (YSB96), *MAT*α *crg1Δ ste50Δ* (YSB632), and *MAT***a** *crg1Δ ste50Δ* (YSB637). Indicated strains were streaked in confrontation with each other on V8 agar medium and incubated at room temperature in the dark. Images were photographed after 10 days. (C) Mating reactions were initiated for the following strains: The *crg1Δ ste50Δ* double mutants showed mating defect in both unilateral crossing and bilateral crossing. *crg1Δ* α × *crg1Δ* **a** (H99 crg1 and PPW 196), *crg1Δ* α × *crg1Δ ste50Δ* **a** (H99 crg1 and YSB637), *crg1Δ ste50Δ* α × *crg1Δ* **a** (YSB632 and PPW 196), *crg1Δ ste50Δ* α × *crg1Δ ste50Δ* **a** (YSB632 and YSB637). The images were photographed after 12 days. (D) Northern blot analysis for monitoring pheromone gene expression was performed with total RNA isolated from solo- or co-cultures of the indicated strain(s) grown for 24 hr under mating conditions: WTα (H99), WT**a** (KN99a), *ste50Δ*α (YSB317), and *ste50Δ***a** (YSB522). The blot was probed with the *MFα1* gene.

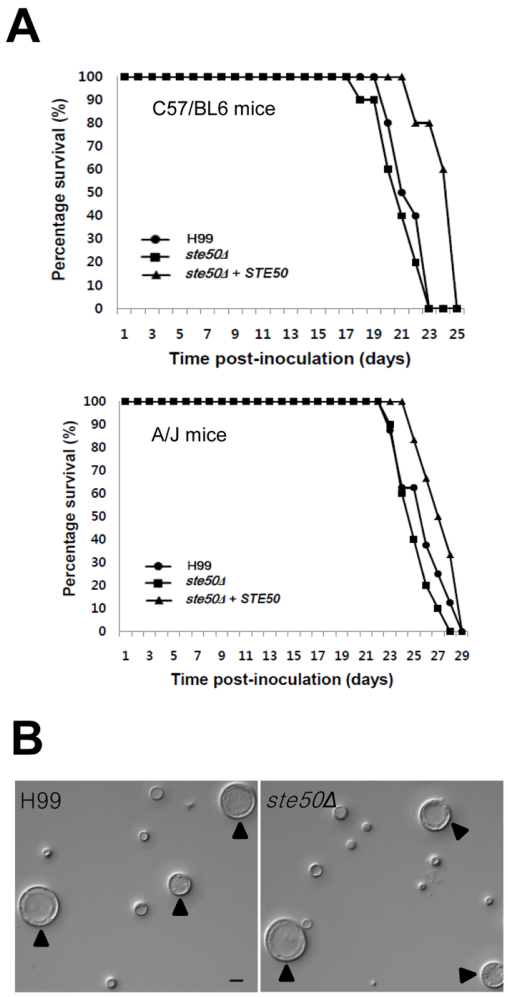

Fig. 7.

Ste50 is dispensable for virulence and titan cell formation of *C. neoformans*. (A) For virulence assays, groups of ten C57/BL6 or groups of six-ten A/J mice (see Materials and Methods) were infected with 5×10^4 cells of *MAT*α WT (●: H99), *ste50Δ* (■: YSB317), and *ste50Δ+STE50* complemented (▲: YSB564) strains by intranasal inhalation. Percent survival (%) was monitored daily until all mice were sacrificed. The *ste50Δ* mutant is as virulent as the WT strain. In both experiments, the *P*-values for the C57/BL6 experiment were: 0.35, 0.001, and 0.001 for H99/*ste50Δ*, *ste50Δ*/*ste50Δ+STE50*, and H99/*ste50Δ+STE50*, respectively. *P*-values for the A/J experiment were 0.57, 0.03, and 0.23 for H99/*ste50Δ*, *ste50Δ*/*ste50Δ+STE50*, and H99/*ste50Δ+STE50*, respectively. (B) For titan cell formation assay, A/J mice were infected with 1×10^6 cells of the wild-type (H99) and *ste50Δ* mutant (YSB317) strains and were sacrificed at 3 days post-infection. Cells in the lung lavage fluid were fixed with 3.7% formaldehyde and photographed. Bar = 10 μm, arrows denote titan cells.

Table 1

Strains used in this study.

Strain	Genotype	Parent	Reference
C. neoformans			
H99	*MAT*α		(Perfect et al., 1993)
KN99**a**	*MAT*a		(Nielsen et al., 2003)
JEC21	*MAT*α		(Moore and Edman, 1993)
JEC20	*MAT*a		(Moore and Edman, 1993)
YSB42	*MAT*α *cac1::NAT-STM#159*	H99	(Bahn et al., 2004)
YSB64	*MAT*α *hog1::NAT-STM#177*	H99	(Bahn et al., 2005b)
YSB81	*MATa hog1::NEO*	KN99**a**	(Bahn et al., 2005b)
YSB313	*MAT*α *ste11::NAT-STM#242*	H99	(Bahn et al., 2007a)
YSB96	*MAT*a *ura5 crg1::URA5 aca1::NEO*	YSB58 × JKH43	(Bahn et al., 2004)
YSB119	*MAT*α *aca1::NAT-STM#43 ura5 ACA1-URA5*	YSB108	(Bahn et al., 2004)
YSB121	*MATa aca1::NEO ura5 ACA1-URA5*	YSB109	(Bahn et al., 2004)
YSB317	*MAT*α *ste50::NAT-STM#296*	H99	This study
YSB318	*MAT*α *ste50::NAT-STM#296*	H99	This study
YSB319	*MAT*α *ste50::NAT-STM#296*	H99	This study
H99 crg1	*M A T*α *ura5 crg1::URA 5*	F99	(Wang et al., 2004)
PPW196	*M A Ta ura5 crg1::URA5*	F99a	(Wang et al., 2004)
YSB523	*MATa ste50::NEO*	KN99**a**	This study
YSB564	*MAT*α *ste50::NAT-STM#296 STE50-NEO- pJAF12*	YSB317	This study
YSB593	*MAT*α *ste50::NAT-STM #224*	JEC21	This study
YSB632	*MAT*α *ste50::NAT-STM #122 ura5 crg1::URA 5*	H99 crg1	This study
YSB637	*MAT*α *ste50::NAT-STM #122 ura5 crg1::URA 5*	PPW196	This study

Each *NAT-STM#* indicates the Nat marker with a unique signature tag.